13. IJTEch2_vol6No.6

by Metta Savitri

Submission date: 13-Apr-2023 08:07AM (UTC-0500)
Submission ID: 2063429557
File name: 13._IJTEch2_vol6No.6.pdf (954.39K)
Word count: 6342
Character count: 25561

International Journal of Technology (2015) 6: 1031-1041
ISSN 2086-9614

AN ANALYSIS OF VOLTAGE SPACE VECTORS' UTILIZATION OF VARIOUS PWM SCHEMES IS DUAL-INVERTER FED FIVE-PHASE OPEN-END WINDING MOTOR DRIVES

I Nyoman Wahyu Satiawan[*,1], Ida Bagus Fery Citarsa[1], I Ketut Wiryajati[1], I Kade Wiratama[2]

[1] *Department of Electrical Engineering, Faculty of Engineering University of Mataram, Mataram 83121, Indonesia*
[2] *Department of Mechanical Engineering, Faculty of Engineering University of Mataram, Mataram 83121, Indonesia*

(Received: July 2015 / Revised: September 2015 / Accepted: October 2015)

ABSTRACT

This paper analyzes voltage space vectors' utilization of various Pulse Width Modulation (PWM) schemes in dual-inverter fed five-phase open-end winding motor drives with equal DC-link voltage. The applied voltage space vectors in three PWM schemes were examined. These three schemes were: the Equal Reference Sharing (ERS) PWM, the Unequal Reference Sharing (URS) PWM, and the Decomposition PWM. The results of these examinations show that the ERS scheme utilizes only 21 of the 211 available voltage vectors, and that the URS scheme utilizes more voltage vectors than the ERS scheme. The number of vectors applied in the URS scheme varies according to the modulation index and angular position of the voltage references. Consequently, the URS scheme produces better voltage output quality than the ERS scheme. Of the three schemes, the Decomposition PWM applies the most effective voltage vectors and produces the best voltage output quality, which is indicated by the lowest value of Total Harmonics Distortion (THD). This paper also proposes a new switching strategy that inherently improves the power sharing capability of the converter, thus avoiding the increase in the DC-link voltage of inverter that operates in PWM mode.

Keywords: Decomposition PWM; Dual-inverter fed five-phase motor; Equal Reference Sharing (ERS); Unequal Reference Sharing (URS)

1. INTRODUCTION

The multi-level inverter is considered to be a promising solution to the limitations on the different rating powers of electronic devices. The availability of the voltage (current) rating of semiconductor devices is currently limited to a view kV (kA) but the power rating of motor may reach to MVA. Conventionally, multi-level inverters have been created by adding two or more switches in the series connection for every inverter leg, and the motor has been fed from one side. More recently, dual-inverter fed open-end winding motor drives were introduced (Stemmler & Guggenbach, 1993). In this structure, the neutral point of the machine is opened, which allows the motor to be supplied from both sides using two inverters.

Dual-inverter fed three-phase drives have been a subject of research for more than two decades (Casadei et al., 2007; Mohapatra et al., 2002; Srinivas & Somasekhar, 2008; Zhao & Lipo, 1995). Extension of the dual-inverter topology into multi-phase drives leads to a significant

* Corresponding author's email: nwahyus@yahoo.com, Tel. +62-370-636126, Fax. +62-370-636523
Permalink/DOI: http://dx.doi.org/10.14716/ijtech.v6i6.1396

increase in complexity, particularly during the development of suitable Pulse Width Modulation (PWM) methods. The complexity rises due to the availability of a large number of voltage space vectors and the existence of multiple two-dimensional (2D) planes.

An effort to develop suitable PWM schemes for the dual-inverter fed five-phase drives was initiated a few years ago (Bodo et al., 2011; Levi et al., 2012; Jones et al., 2011; Jones et al., 2012; Jones & Satiawan, 2012; Satiawan & Jones, 2011). Two PWM schemes were developed based on the method for apportioning voltage references; these are known as the Equal Reference Sharing (ERS) PWM and the Unequal Reference Sharing (URS) PWM schemes (Jones & Satiawan, 2012; Levi et al., 2012). Further, a PWM scheme called Decomposition PWM was developed by decomposing the voltage space vectors' decagon into several smaller decagons that were equivalent to a two-level inverter (Jones et al., 2011; Jones et al., 2012; Satiawan & Jones, 2011). PWM schemes based on the carrier-based method for the dual-inverter fed five-phase drive are discussed in a study by Bodo et al. (2011). Meanwhile, a comparison of the performances of various PWM schemes for the dual-inverter fed five-phase drive is presented in a study by Satiawan et al. (2014). It is revealed in Satiawan et al. (2014) that the Decomposition PWM scheme generates the best voltage output quality of the three PWM schemes, as indicated by its low Total Harmonics Distortion (THD) value.

The available PWM schemes of the dual-inverter fed five-phase motor drives were developed based on the voltage space vectors of the individual two-level inverters, which are modulated according to respective voltage references that are apportioned to the two inverters. This paper investigates the voltage space vectors' utilization of various PWM schemes in the dual-inverter fed five-phase motor drives. It does so from the perspective of single three-level voltage space vectors. Information regarding applied voltage vectors can be used to further improve converter performance. This paper also proposes a new switching strategy that inherently improves the power-sharing capability of the converter. This new switching strategy utilizes the redundant switching states in the applied vectors; thus, both inverters alternate between operating in PWM mode and clamping mode. The simulation result of the new switching strategy PWM confirms that the DC-link voltage of both inverters is maintained at 300 V for all speed ranges.

2. EXPERIMENTAL PROCESS

2.1. Voltage Space Vectors of the Dual-inverter Fed Five-phase Motor Drives

Figure 1 shows a simplified wiring diagram of a dual-inverter fed five-phase open-end winding motor drive. This diagram shows how the five-phase motor is supplied from both sides by two two-level inverters. Based on the notation given in Figure 1, the voltages of phase stator windings v_{xs} $(x = a, b, c, d, e)$ can be given as:

$$\begin{aligned} v_{as} &= (v_{A1N1} + v_{N1N2} - v_{A2N2}) \\ v_{bs} &= (v_{B1N1} + v_{N1N2} - v_{B2N2}) \\ v_{cs} &= (v_{C1N1} + v_{N1N2} - v_{C2N2}) \\ v_{ds} &= (v_{D1N1} + v_{N1N2} - v_{D2N2}) \\ v_{es} &= (v_{E1N1} + v_{N1N2} - v_{E2N2}) \end{aligned} \tag{1}$$

where v_{X1N1} $(_{X=A,B,C,D,E})$ and v_{X2N2} $(_{X=A,B,C,D,E})$ are the leg voltages of inverter 1 and inverter 2, respectively, and v_{N1N2} is the common mode voltage.

A five-phase machine can be modeled in two 2D subspaces; these are the so-called α-β and x-y sub-spaces (Zhao & Lipo, 1995). In a machine with nearly sinusoidal magneto-motive force, only harmonics components mapped in α-β plane are able to develop useful torque, while the

harmonics mapped in *x-y* plane relate to the motor losses (copper losses and friction losses). The development of a PWM strategy must therefore simultaneously consider both 2D subspaces (Levi, 2008). The two-level five-phase inverter has 32 (2^5) switching states.
Using (1) and (2), these 32 switching states produce 31 voltage space vectors that are mapped in two 2D planes, as shown in Figure 2. The decimal number in the vectors in Figure 2 indicates the switching function of the upper switches of the phase-inverter leg when these switches are converted into binary (Dujic et al., 2009).

$$\underline{v}_{\alpha\beta} = v_\alpha + jv_\beta = 2/5(v_a + \underline{a}v_b + \underline{a}^2 v_c + \underline{a}'^2 v_d + \underline{a}' v_e) \tag{2}$$

$$\underline{v}_{xy} = v_x + jv_y = 2/5(v_a + \underline{a}^2 v_b + \underline{a}' v_c + \underline{a}v_d + \underline{a}'^2 v_e) \tag{3}$$

where $\underline{a} = \exp(j2\pi/5)$, $\underline{a}^2 = \exp(j4\pi/5)$, $\underline{a}' = \exp(-j2\pi/5)$, $\underline{a}'^2 = \exp(-j4\pi/5)$

v_{xs} ($x = a, b, c, d, e$) are the voltage of the phase stator windings. By substituting (1) with (2) and (3), and by knowing $v_{N1N2}(1 + \underline{a} + \underline{a}^2 + \underline{a}'^2 + \underline{a}') = 0$, the phase voltage space vectors of the dual-inverter fed five-phase motor drive can be derived as:

$$\begin{aligned}\underline{v}_{\alpha\beta(DUAL)} = 2/5\{&(v_{A1N1} - v_{A2N2}) + \underline{a}(v_{B1N1} - v_{B2N2}) + \underline{a}^2(v_{C1N1} - v_{C2N2}) \\ &+ \underline{a}'^2(v_{D1N1} - v_{D2N2}) + \underline{a}'(v_{E1N1} - v_{E2N2})\end{aligned} \tag{4}$$

$$\begin{aligned}\underline{v}_{xyDUAL)} = 2/5\{&(v_{A1N1} - v_{A2N2}) + \underline{a}^2(v_{B1N1} - v_{B2N2}) + \underline{a}'(v_{C1N1} - v_{C2N2}) \\ &+ \underline{a}'(v_{D1N1} - v_{D2N2}) + \underline{a}'^2(v_{E1N1} - v_{E2N2})\end{aligned} \tag{5}$$

Equations 4 and 5 designate that the voltage space vectors of the dual-inverter fed structure are governed by the leg voltages of inverter 1, v_{X1N1}($_{X=A,B,C,D,E}$), and the leg voltages of inverter 2, v_{X2N2} ($_{X=A,B,C,D,E}$). The resulting space vectors in the dual-inverter fed structure depend on the DC-link voltage ratio of the two inverters. When the equal DC-link is applied, the 1024 (32×32) switching state combinations will map 211 voltage space vectors in both *α-β* and *x-y* planes, as shown in Figure 3. The mapping of the voltage space vectors is equal to that of three-level voltage space vectors in single-sided five-phase supply drives (Levi et al., 2010). In this case, one or more switching states may be mapped in the same voltage vector; these states are then known as redundant switching states.

2.2. Development of the New Switching Strategy

The utilized voltage vectors of the PWM schemes are traced from the switching pulses of the upper switches of inverter 1 and inverter 2. Using a simple MATLAB code, the switching trajectory at a specific angular position and modulation index can be determined, and the position of the related vectors in both planes can then be identified. For the sake of clarity, the modulation index is defined as $M = v^{**}/(0.5V_{dc})$, where v^{**} is the modulating reference voltage and V_{dc} is the value of the DC-link voltage of an individual inverter.

Based on the information from the utilized vectors, a new switching strategy is proposed. The new switching technique is developed by applying the specific redundant switching states to the applied voltage vectors. Using a different set of switching states, a new switching sequence is achieved; this sequence can direct the two inverters to operate interchangeably between PWM mode and clamping mode, as opposed to operating one inverter in PWM mode and another inverter in square wave mode/clamping mode (as in the case of the Decomposition PWM scheme)

3. RESULTS AND DISCUSSION

3.1. Evaluation of the Applied Voltage Space Vectors of the ERS PWM Scheme

The switching trajectory of the ERS PWM when the voltage reference is placed at an angular position of $\theta = 0 - 36°$ (Sector 1), as well as the related switching sequences, are shown in the upper trace of Figure 4.

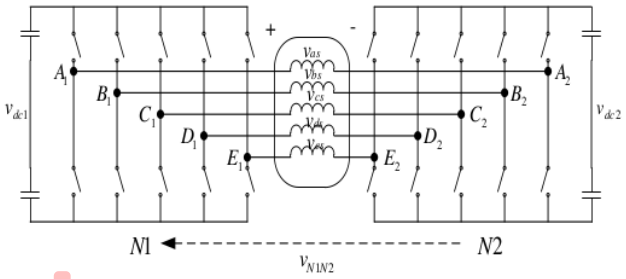

Figure 1 The structure of the dual two-level inverter fed a five-phase open-end winding motor drive

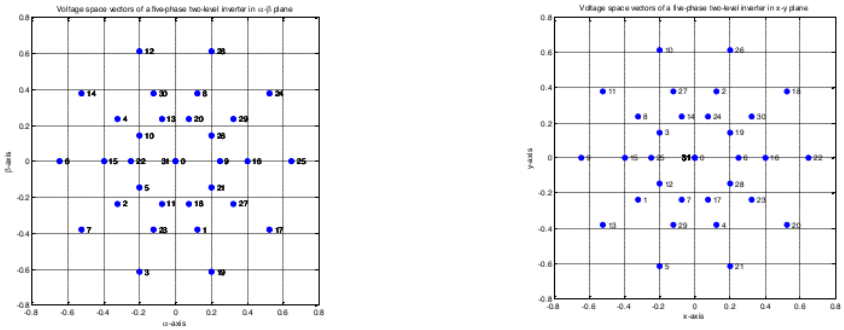

Figure 2 Voltage space vectors of a five-phase two-level Voltage Source Inverter (VSI) in the α-β and x-y planes

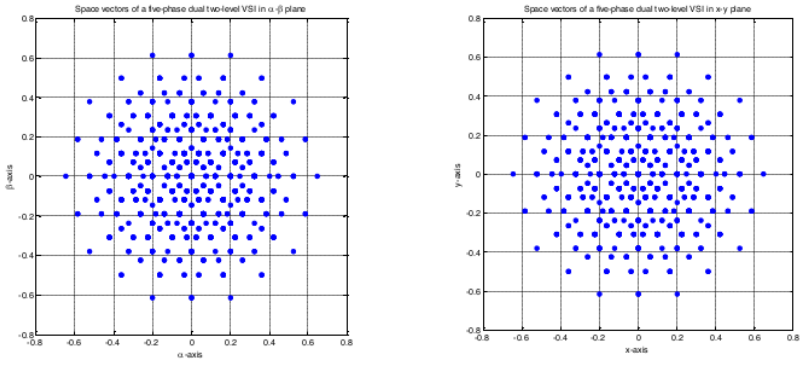

Figure 3 The mapping of voltage space vectors of a dual-inverter fed five-phase drive for equal DC-link voltages in the α-β and x-y planes

The label of the vectors indicates the switching function of the upper switches when those switches are converted into binary. It can be seen that six switching state combinations are

applied in Sector 1, and that these combinations relate to five voltage vectors. The switching sequence in Sector 1 indicates that the switches of inverter 1 are activated in the opposite manner with respect to the switches of inverter 2. The related voltage vectors that are utilized by the ERS PWM for both the α-β and x-y planes are shown in the lower trace of Figure 4. The ERS PWM scheme only applies 21 of the 211 voltage vectors. This means that the available voltage vectors cannot be optimally applied for generating the output voltage. The applied vectors are only governed by the angular position of the reference (sector), and these vectors are unrelated to the magnitude of the voltage reference. The utilized vectors in the ERS PWM scheme are similar to those used in the two-level single-side inverter. Thus, the quality of the output voltages in the ERS scheme is equivalent to the quality of the output voltages of the conventional two-level inverter.

3.2. Evaluation of the Applied Voltage Space Vectors of the URS PWM Scheme

Before the utilized voltage vectors can be discussed, the sub-sector division of the URS and Decomposition PWM schemes must first be defined. To identify the sub-sectors, the method developed by Gao and Fletcher (2010) can be used. Alternatively, the division of sub-sectors is determined by examining the intersection of the five voltage references. The borderlines of the sub-sectors can be deduced from the intersection of the references. The intersection of the references results in the subsector division, as shown in Figure 5a. It is shown in Figure 5a that one sector with a span of 36° is divided into 13 sub-sectors. Likewise the intersection of the references in the Decomposition PWM also divides one sector with a span of 36° into 13 sub-sectors as shown in Figure 5 b.

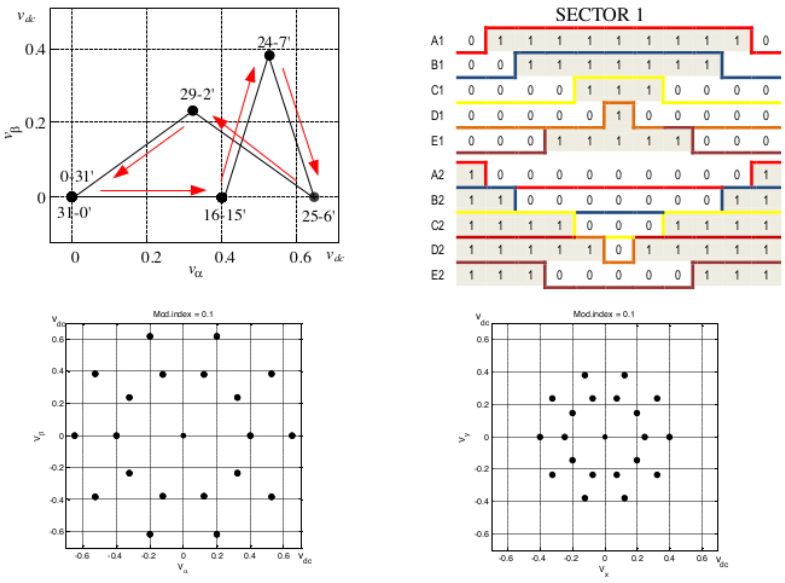

Figure 4 Upper trace: the switching trajectory and related switching sequence of the PWM scheme in Sector 1. Lower trace: the applied voltage space vectors in the ERS PWM scheme for both the α-β and x-y planes

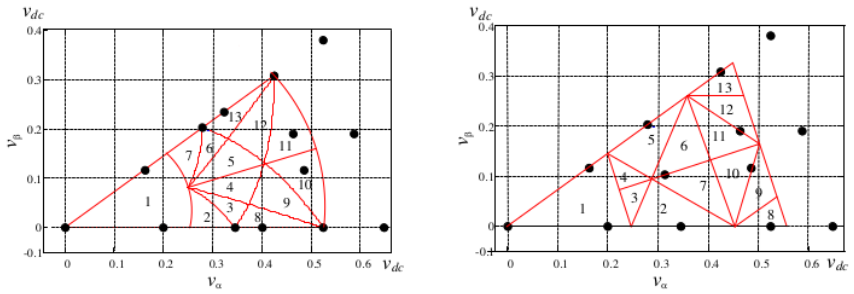

(a) (b)

Figure 5 The sub-sector division of sector 1 and the applied space vectors for: (a) the URS PWM, and (b) the Decomposition PWM

The switching trajectories and the related switching sequences (for one half of the switching period) of the URS PWM scheme at a specific modulation index of M = 0.8 and an angular position of θ = 9° (sub-sector 9) are shown in Figure 6 (a). While the switching trajectories and the related switching sequences at M = 0.5 and θ = 0–36° (sector 1) are shown in Figure 6b.

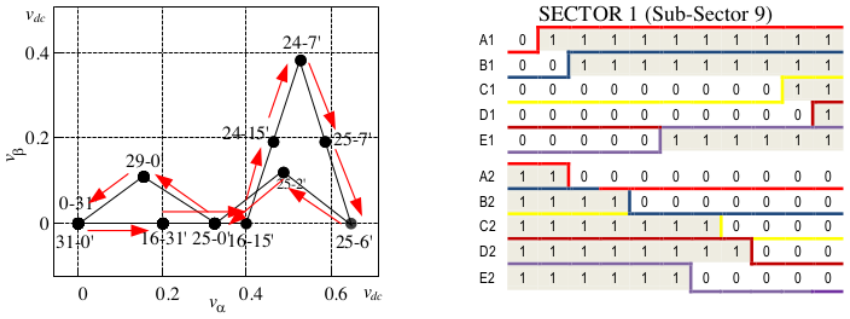

(a)

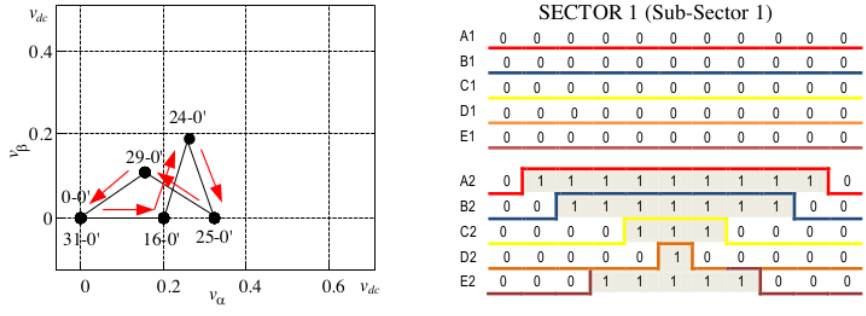

(b)

Figure 6 The switching trajectory and the related switching sequence of the URS PWM scheme at: (a) M = 0.8 in subsector 9; (b) M = 0.5 in sector 1

Figure 6a shows that at subsector 9, the modulators employ 11 switching state combinations that are mapped as 10 voltage vectors. The switching sequence indicates that both inverters operate in PWM mode, but that they do not work in a complimentary manner. Meanwhile,

Figure 6b shows that at $M = 0.5$ (sector 1), 6 switching state combinations are applied; these all relate to 5 voltage vectors. The switching sequence shows that only one inverter is activated while the other inverter is clamped at zero vector. Further investigation reveals that the applied voltage vectors vary according to modulation index, as shown in Figure 7 for both the α-β and x-y planes. The triggered vectors in the URS scheme at $M = 1.05$ (max) are the same as those used by the ERS scheme (which utilizes 21 vectors). When $M = 0.5$, the number applied vectors is also 21. The magnitude of the applied vectors at $M = 0.5$ are smaller than the used vectors at $M = 1.05$. When $M = 0.8$ and $M = 0.6$, the URS PWM scheme utilizes 71 vectors. Among those 71 vectors, there are 10 vectors that are applied at $M = 0.8$; these are different than those applied at $M = 0.6$. Because more vectors are applied, the performance of the URS scheme is better than that of the ERS scheme (except at $M = 1.05$, where the performance is exactly the same). This result indicates that the performance of the inverter is closely related to the vectors that are applied in the PWM schemes.

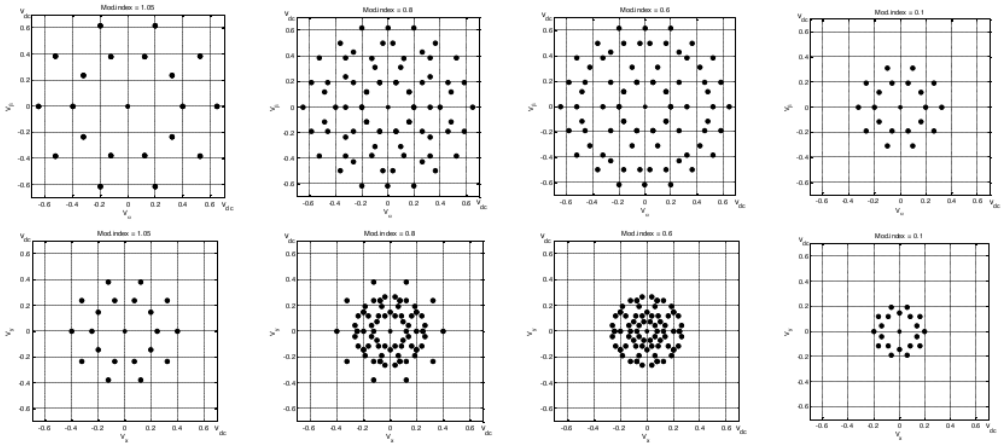

(a) $M = 1.05$ (b) $M = 0.80$ (c) $M = 0.60$ (d) $M = 0.50$

Figure 7 The applied voltage vectors in the URS PWM scheme at various modulation indices for both the α-β (upper trace) and x-y planes (lower trace)

3.3. Evaluation of the Applied Voltage Space Vectors of the Decomposition PWM Scheme

The switching trajectories of the Decomposition PWM at $M = 1.05$, $\theta = 9°$ (subsector 9), and $\theta = 27°$ (subsector 12), as well as the respective switching sequences, are shown in Figure 8. The Decomposition PWM applies six switching state combinations that are mapped in five voltage vectors for each subsector, and no zero vectors are triggered. The switching sequences show that the two inverters operate in different PWM modes, one inverter operates in PWM mode, and one inverter is clamped in a specific switching state. The mapping of the applied voltage vectors in the α-β and x-y planes for $M = 1.05$, $M = 0.6$, and $M = 0.5$ are shown in Figure 9. Figure 9 indicates that the number of active vectors utilized by the converter varies even more than the vectors applied in the ERS and URS PWM schemes. The number of applied vectors is governed by the value of the modulation index. There are 40 active vectors applied when $M = 0.6$. When the modulation index is set to its maximum ($M = 1.05$), the number of applied vectors further increases to 60 active vectors. At $M = 0.5$, the number of applied vectors is the same as the number of applied vectors in the URS PWM (21 vectors). In cases of $M > 0.525$, vectors of zero were not applied, and the mapping of the applied vectors in the x-y plane indicates that no large vectors are triggered. As a result, the number of levels in the phase

voltage increases significantly, which leads to improvement in the quality of both the voltage and the current. In addition, the absence of the zero vectors in the present study is consistent with the three-level single-sided output waveforms found in previous research (Gao & Fletcher, 2010). This is contrary to the URS scheme, where the zero vectors are always applied throughout the operating range, including when the VSI operates in multi-level mode, therefore resulting in pseudo-multi-level voltage waveforms.

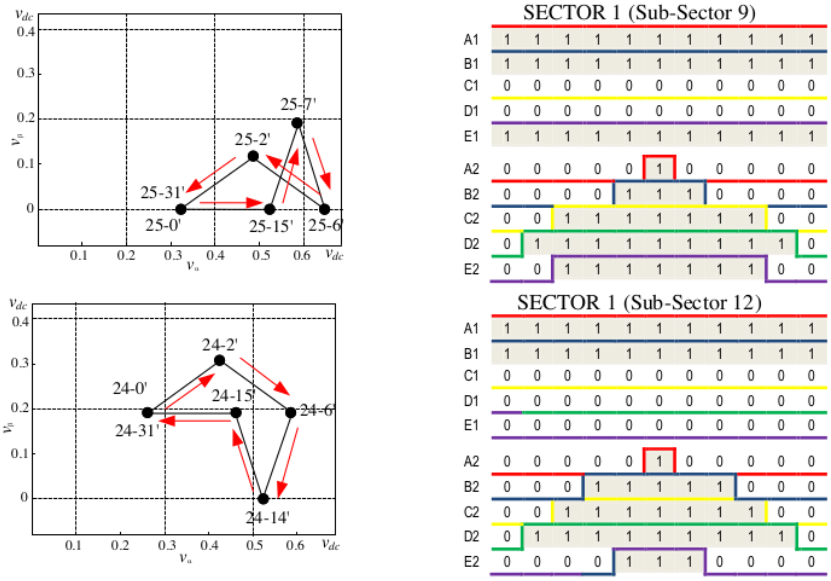

Figure 8 The switching trajectory and the related switching sequence of the Decomposition PWM scheme at M = 1.05 of subsector 9 (upper trace) and M = 1.05 of subsector 12 (lower trace)

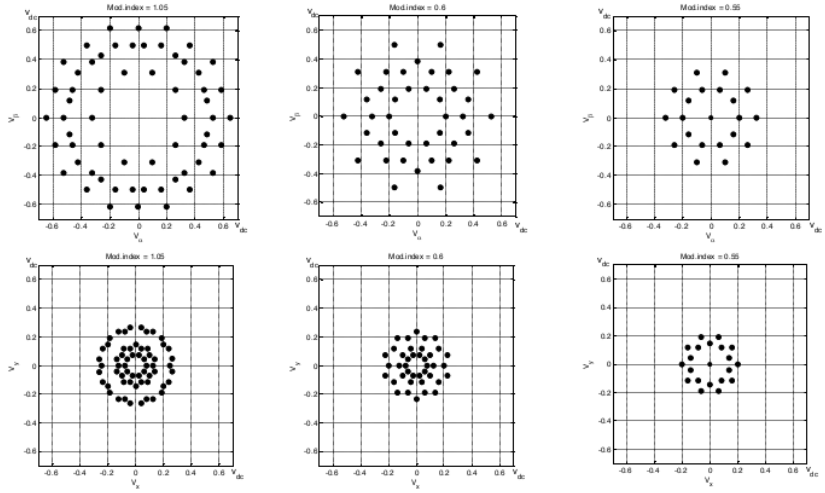

(a) M = 1.05 (b) M = 0.60 (c) M = 0.5

Figure 9 The applied voltage vectors in the Decomposition PWM scheme at various modulation indices for both the α-β (upper trace) and x-y planes (lower trace)

3.4. Proposed Switching Strategy for the Decomposition PWM Scheme

Of the three PWM schemes, the Decomposition PWM scheme is able to generate the best output voltage (Satiawan et al., 2014). However, the Decomposition PWM scheme may suffer from the unbalance condition, particularly at a modulation index of $0.525 < M < 0.638$. The unbalance condition occurs when the load requires less power than the power produced by one inverter operating in square wave mode. The excessive power produced by that one inverter is then transferred to the other inverter. This condition causes the DC-link voltage of inverter that operated in PWM mode increases, thereby affecting the converter's performance (Jones et al., 2012).

To avoid the increase in DC-link voltage of the PWM inverter the ratio of DC-link voltage is adjusted to a certain value so that the power produced by the square wave inverter is the same or less than the power required by the load (Jones et al., 2012). Another method for solving the voltage increase problem is to develop a new switching technique that interchangeably alternates the operation of the two inverters between PWM mode and square wave mode. This technique has been successfully applied to a three-phase drive system (Srinivas & Somasekhar, 2008). The switching sequences of the proposed switching strategy at $M = 1.05$, $\theta = 9$ (subsector 9), and $\theta = 27$ (subsector 12) are shown in Figure 10. The new switching strategy exposes the redundant switching vectors that are available in this structure.

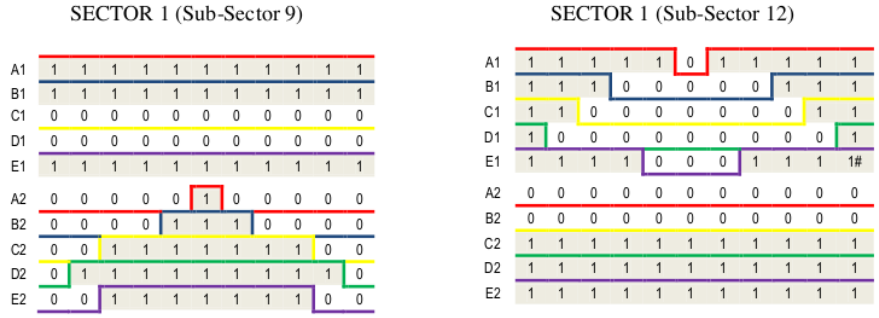

Figure 10 The proposed switching sequences of the Decomposition PWM scheme at $M = 1.05$ of subsector 9 (left) and $M = 1.05$ of subsector 12 (right)

Figure 10 shows how when the reference lays at subsector 9, inverter 1 is clamped at a switching state of 11001 (25) and inverter 2 operates in PWM mode. Subsequently, when the reference moves to subsector 12, inverter 1 goes into PWM mode and inverter 2 is clamped in a switching state of 00111 (7). By applying this switching technique, the capability of the two inverters in sharing the load power equally is maintained for all ranges of modulation indices; hence, the increase of DC-link voltage at a particular speed range is avoided. Figure 11 shows the value of the DC-link voltages of both inverters at $M = 0.6$.

The new switching strategy is able to maintain the DC-link voltages at the desired value. In contrast, at $M = 0.6$, the original switching technique of the decomposition PWM fails to keep the DC-link voltage at the desired level. It is also worth mentioning that the utilized voltage vectors in the new switching strategy are exactly the same as those used in the original Decomposition PWM scheme.

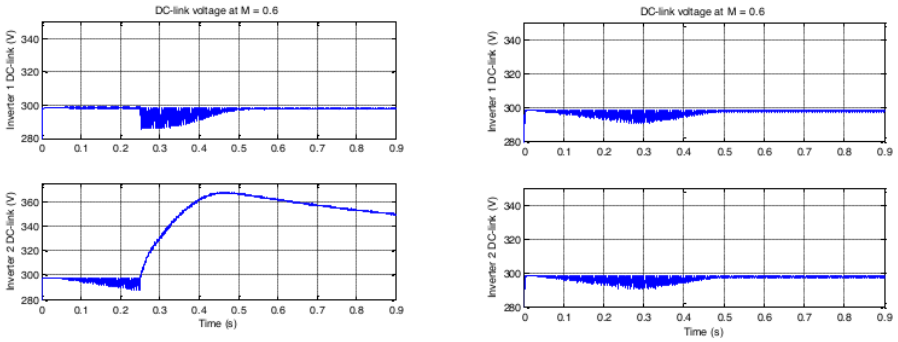

Figure 11 The inverter DC-link voltages at $M = 0.6$ for the Decomposition PWM (left) and the Decomposition PWM with new switching strategy (right)

4. CONCLUSION

This paper discusses the voltage space vectors' utilization of the three PWM schemes in the dual-inverter fed five-phase open-end winding drives. The utilized voltage vectors are traced using a combination of switching pulses from the upper switches of inverter 1 and the switching pulses of the upper switches of inverter 2. The results show that the Decomposition PWM scheme is able to utilize the most effective voltage vectors, hence enabling the synthesizing of output voltages closer to the voltage references, in comparison to the ERS and URS PWM schemes. In both the Decomposition and URS PWM schemes, the applied voltage vectors vary according to the angular position and magnitude of the reference (i.e., the modulation index). In contrast, the ERS PWM scheme utilizes only 21 of the 211 available vectors, which are equivalent to the vectors used in the two-level inverter. Meanwhile, the URS scheme involves the largest number of vectors, but these vectors have a poorer ability in synthesizing nearly sinusoidal voltages than the vectors used by the Decomposition PWM scheme. As a consequence, the Decomposition PWM has the best performance among the three PWM schemes. This confirms that the ability of the PWM scheme to apply the most accurate voltage vectors has a significant effect on the performance of the converter. Based on the aforementioned results, a new switching strategy is proposed to further enhance the converter's performance, particularly in terms of improving the power-sharing capability between the two inverter.

5. REFERENCES

Bodo, N., Levi, E., Jones, M., 2011. Carrier-based Modulation Techniques for Five-phase Open-end Winding Drive Topology. In: *Proceedings of the IEEE Industrial Electronics Annual Conference (IECON)*. Melbourne, 7-10 November, Australia

Casadei, D., Grandi, G., Lega, A., Rossi, C., Zarri, L., 2007. Switching Technique for Dual-two Level Inverter Supplied by Two Separate Sources. In: *Proceedings of the IEEE Applied Power Electronics Conference (APEC)*. Anaheim, California, 28 February, USA

Dujic, D., Jones, M., Levi, E., 2009. Generalized Space Vector PWM for Sinusoidal Output Voltage Generation with Multi-phase Voltage Source Inverters. *International Journal of Industrial Electronics and Drives,* Volume 1(1), pp. 1–13

Gao, L., Fletcher, J.E., 2010. A Space Vector Switching Strategy for Three-level Five-phase Inverter Drives. *IEEE Transactions on Industrial Electronics*, Volume 57(7), pp. 2332–2343

Jones, M., Satiawan, I.N., 2012. A Simple Multi-level Space Vector Modulation Algorithm for

Five-phase Open-end Winding Drives. *Transactions on International Association for Mathematics and Computers in Simulation (IMACS)* Journal, Volume 90, pp. 74–85

Jones, M., Satiawan, I.N., Bodo. N., Levi, E., 2012. A Dual Five-phase Space-vector Modulation Algorithm based on the Decomposition Method. *IEEE Transactions on Industry Applications,* Volume 48(6), pp. 1–11

Jones, M., Satiawan, I.N., Levi, E., 2011. A Three-level Five-phase Space-vector Modulation Algorithm based on the Decomposition Method. In: *Proceedings of the IEEE International Electric Machines and Drives Conference (IEMDC)*. Niagara Falls, 15-18 May, Canada

Levi, E., 2008. Multi-phase Electric Machines for Variable-speed Applications. *IEEE Transactions on Industrial Electronics*, Volume 55(5), pp. 1893–1909

Levi, E., Jones, M., Satiawan, W., 2010. A Multi-phase Dual-inverter Supplied Drive Structure for Electric and Hybrid Electric Vehicles. In: *Proceedings of the IEEE Vehicle Power and Propulsion Conference (VPPC)*. Lille, 1-3 September, France

Levi, E., Satiawan, I.N., Bodo, N., Jones, M., 2012. A Space-vector Modulation Scheme for Multilevel Open-end Windings Five-phase Drives. *IEEE Transactions on Energy Conversion,* Volume 27(1), pp. 1–10

Mohapatra, K.K., Somasekhar, V.T., Gopakumar, K., 2002. A Harmonic Elimination Scheme for an Open-end Winding Induction Motor Drive Fed from Two Inverters using Asymmetrical D.C. Link Voltages. European Power Electronics and Drives (EPE) Journal, Volume 12(4), pp. 28–36

Satiawan, I.N., Citarsa, I.B., Wiryajati, I.K., Aware, M.A., 2014. Performance Comparison of PWM Schemes of Dual-inverter Fed Five-phase Motor Drives. *International Journal of Technology,* Volume 5(3), pp. 277–286

Satiawan, W., Jones, M., 2011. A Multi-frequency PWM Scheme for Multi-level Five-phase Open-end Winding Drives. In: *Proceedings of the Universities' Power Engineering Conference (UPEC)*. Soest, 5-8 September, Germany

Srinivas, S., Somasekhar, V.T., 2008. Space Vector Based PWM Switching Strategies for a Three-level Dual-inverter Fed Open-end Winding Induction Motor Drives and their Comparative Evaluation. IET Transactions on Electrical Power Applications, Volume 2(1), pp. 19–31

Stemmler, H., Guggenbach, P., 1993. Configurations of High-power Voltage Source Inverter Drives. In: *Proceedings of the European Power Electronics and Applications Conference (EPE)*. Brighton, 13–18 September, UK

Zhao, Y., Lipo, T.A., 1995. Space Vector PWM Control of Dual Three-phase Induction Machine using Vector Space Decomposition. IEEE Transactions on Industry Applications, Volume 31(5), pp. 1100–1109

13. IJTEch2_vol6No.6

ORIGINALITY REPORT

17%	12%	13%	4%
SIMILARITY INDEX	INTERNET SOURCES	PUBLICATIONS	STUDENT PAPERS

MATCH ALL SOURCES (ONLY SELECTED SOURCE PRINTED)

2%

★ www.sciencepubco.com

Internet Source

Exclude quotes	On	Exclude matches	Off
Exclude bibliography	On		

13. IJTEch2_vol6No.6

GRADEMARK REPORT

FINAL GRADE

/0

GENERAL COMMENTS

Instructor

PAGE 1

PAGE 2

PAGE 3

PAGE 4

PAGE 5

PAGE 6

PAGE 7

PAGE 8

PAGE 9

PAGE 10

PAGE 11